*Int. J. Heat Mass Transfer.* Vol. 35, No. 4, pp. 741–748, 1992
Printed in Great Britain

0017-9310/92 $5.00+0.00
Pergamon Press plc

# Buoyancy driven convection in a rectangular enclosure with a transverse magnetic field

J. P. GARANDET and T. ALBOUSSIERE
CEA/IRDI/CEREM/DEM, Section d'Etude de la Solidification et de la Cristallogénèse, Centre d'Etudes Nucléaires de Grenoble, 85 X, 38041 Grenoble Cedex, France

and

R. MOREAU
INPG Laboratoire Madylam UA CNRS 1326, ENSHMG, BP 95, 38402 St Martin d'Heres Cedex, France

(*Received* 5 *February* 1990 *and in final form* 3 *May* 1991)

**Abstract**—We propose an analytical solution to the equations of magnetohydrodynamics that can be used to model the effect of a transverse magnetic field on buoyancy driven convection in a two-dimensional cavity. In the high Hartmann number limit, the velocity gradient in the core is constant outside of the two Hartmann layers at the vicinity of the walls normal to the magnetic field. We show that this core solution is correct everywhere in the cavity except in a boundary layer of extent $Ha^{-1/2}$ at the cold wall. The recirculating part of the flow is studied by means of a series expansion that allows for the computation of the stream function. We also present the variation of both components of velocity as a function of *Ha*, along with a discussion of the validity of our assumptions.

## 1. INTRODUCTION

CONVECTION is an important parameter in crystal growth experiments from the melt as it can account for both heat and mass transfer in the liquid phase. It is well known that these unavoidable hydrodynamic movements can be damped with the help of a magnetic field (see for instance refs. [1, 2]). This effect has been thoroughly studied in the past few years in the Czochralski configuration [3–8]. Comparatively little attention has been paid to the Bridgman technique which is also of interest for solidification, both on the ground and in microgravity [9–11]. A pendent question is to know whether diffusive solute transport conditions can be achieved on earth with the help of a magnetic field. In this paper, we propose a two-dimensional solution to the equations of the magnetohydrodynamics that can be used to model the horizontal Bridgman method. To do so, we extend the work of Hart [12, 13] and Birikh [14] to the case where a magnetic field is present.

## 2. BACKGROUND

The fluid is contained in a cavity of infinite extent along the $Y$ direction; the lateral ends are maintained at temperatures $T_0$ and $T_0+\Delta T$ respectively and the applied magnetic field $B_0$ is parallel to gravity (see Fig. 1). Neglecting the effect of Joule heating and viscous dissipation on heat transfer and also assuming that the induced magnetic field is very small compared

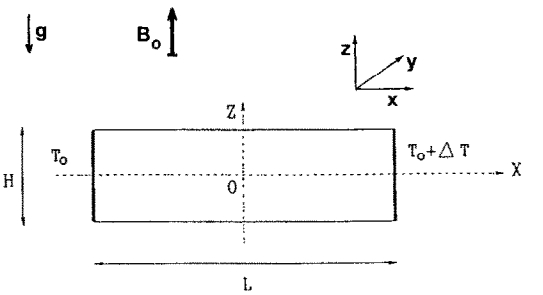


FIG. 1. Geometry of the problem and coordinates; the cavity is supposed infinite in the $Y$-direction.

to $B_0$, the equations of the problem are, in the Boussinesq approximation:

continuity

$$\nabla\cdot\mathbf{V}=0 \tag{1}$$

momentum transfer

$$\frac{\partial\mathbf{V}}{\partial t}+(\mathbf{V}\cdot\nabla)\mathbf{V}=-\frac{1}{\rho_0}\nabla P+\frac{1}{\rho_0}\mathbf{j}\mathbf{x}\mathbf{B}_0 +\nu\nabla^2\mathbf{V}-\beta(T-T_0)\mathbf{g} \tag{2}$$

heat transfer

$$\frac{\partial T}{\partial t}+(V\cdot\nabla)T=\alpha\nabla^2T \tag{3}$$

electric charge transfer

$$\nabla\cdot\mathbf{j}=0 \quad \mathbf{j}=\sigma(-\nabla\phi+\mathbf{V}\mathbf{x}\mathbf{B}_0). \tag{4}$$

## NOMENCLATURE

| | |
|---|---|
| $B_0$ | applied magnetic field |
| $g$ | intensity of gravity |
| $H$ | cavity height |
| **j** | electric current |
| $L$ | cavity length |
| $P$ | pressure |
| $T$ | temperature |
| $T_0$ | minimum temperature of the liquid |
| $U$, $W$ | $X$, $Z$ components of the velocity |
| $u$, $w$ | non-dimensional values of $U$, $W$ |
| $u_M$, $w_M$ | maximum non-dimensional velocities for $u$, $w$ |
| **V** | velocity vector |
| $X$, $Y$, $Z$ | dimensional coordinates |
| $x$, $y$, $z$ | non-dimensional coordinates |
| **x, y, z** | unit vectors. |

Greek letters

| | |
|---|---|
| $\alpha$ | thermal diffusivity |
| $\beta$ | coefficient of thermal expansion |
| $\Delta T$ | temperature difference between the lateral ends of the cavity |
| $\varepsilon$ | aspect ratio of the cavity, $H/L$ |
| $\vartheta$ | non-dimensional temperature field |
| $\nu$ | kinematic viscosity |
| $\rho_0$ | density at temperature $T_0$ |
| $\sigma$ | electrical conductivity |
| $\Phi$ | electric potential |
| $\psi$ | stream function of velocity. |

Non-dimensional parameters

| | |
|---|---|
| $Gr$ | Grashof number, $\beta g(\Delta T/L)H^4/\nu^2$ |
| $Ha$ | Hartmann number, $B_0 H(\sigma/\rho_0\nu)^{1/2}$ |
| $Pr$ | thermal Prandtl number, $\nu/\alpha$. |

In the above equation, $\phi$ stands for the electric potential and $-\nabla\phi$ for the associated electric field. From now on, we assume that all the variables are time independent. Equations (4) then become

$$\Delta\phi - B_0(\partial U/\partial Y - \partial V/\partial X) = 0.$$

In our two-dimensional frame, we are left with a harmonic equation for the electric potential, $\Delta\phi = 0$, which is valid in the melt as well as in the neighbouring solid media. Since there is always somewhere around the enclosure an electrically insulating boundary on which $\partial\phi/\partial n = 0$, the unique solution is $\nabla\phi = 0$, which means that the electric field vanishes everywhere. The Lorentz force then reduces to a systematically damping factor $-B_0^2 U\mathbf{x}$. This situation is similar to that of pressure driven flows in a 2D perfectly conducting duct. Overvelocity effects as predicted by Hunt [15] can only be observed in more complex 3D problems.

## 3. THE CORE SOLUTION

### 3.1. *Outline of the solution*

Let us first look at the velocity field in the core of the cavity. We will look for a solution of the form $\mathbf{V} = U(Z)\mathbf{x}$ that automatically satisfies the continuity equation. Projection of equations (2) on the coordinate axis leads to

$$\frac{-1}{\rho_0}\frac{\partial P}{\partial X} - \frac{1}{\rho_0}\sigma B_0^2 U + \nu\frac{\mathrm{d}^2 U}{\mathrm{d}Z^2} = 0 \tag{5}$$

$$\frac{-1}{\rho_0}\frac{\partial P}{\partial Z} + \beta g(T - T_0) = 0. \tag{6}$$

The boundary conditions of the velocity problem are:

$$U = 0 \quad \text{at } Z = \pm H/2 \text{ (no slip)}$$

$$\text{and at } Z = 0 \text{ (symmetry)}.$$

As for temperature, following Hart [12], we will study two different cases:

thermally insulating walls

$$\frac{\partial T}{\partial Z} = 0 \quad \text{at } Z = \pm H/2;$$

thermally conductive walls

$$T = \frac{\Delta T}{L}X \quad \text{at } Z = \pm H/2.$$

As shown by Birikh [14], the axial temperature gradient in the cavity is constant, $\partial T/\partial X = \Delta T/L$. Elimination of pressure between equations (5) and (6) yields

$$\nu\frac{\mathrm{d}^3 U}{\mathrm{d}Z^3} - B_0^2\frac{\sigma}{\rho_0}\frac{\mathrm{d}U}{\mathrm{d}Z} = \beta g\frac{\Delta T}{L}. \tag{7}$$

Let us now rewrite the equations using reduced variables, defined as

$$x = X/H, \quad z = Z/H, \quad u = HU/\nu, \quad \vartheta = (T - T_0)/\Delta T.$$

The non-dimensional groups appearing in the equations are the thermal Prandtl number $Pr_T = \nu/\alpha$, the Grashof number $Gr = \beta g(\Delta T/L)H^4/\nu^2$, the Hartmann number $Ha = B_0 H(\sigma/\rho_0\nu)^{1/2}$, and the aspect ratio of the cavity $\varepsilon = H/L$. Equation (7) now becomes

$$\frac{\mathrm{d}^3 u}{\mathrm{d}z^3} - Ha^2\frac{\mathrm{d}u}{\mathrm{d}z} = Gr. \tag{8a}$$

Equation (3) becomes, in non-dimensional form

$$\frac{\mathrm{d}^2\vartheta}{\mathrm{d}z^2} = Pr_T\,\varepsilon u. \tag{8b}$$

Taking into account the boundary conditions, the solution to equation (8a) is

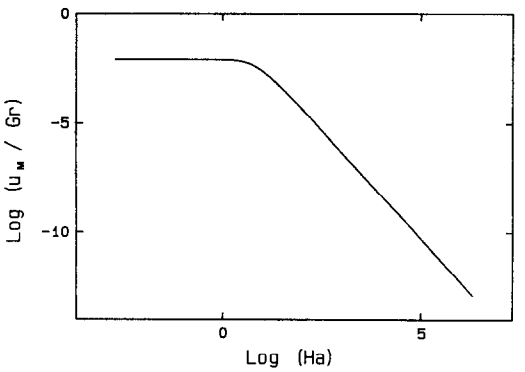


FIG. 2. Variation of the maximum velocity of the fluid in the core, normalized by $Gr$, as a function of $Ha$.

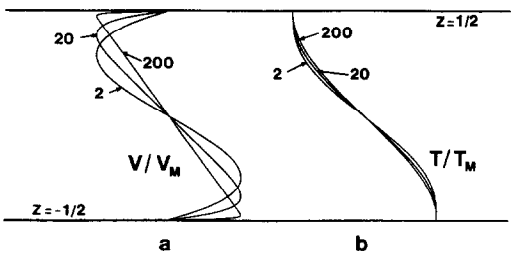


FIG. 3. Normalized velocity (a) and temperature (b) profiled across the cavity for values of the Hartmann number $Ha = 2$, 20 and 200. Temperature distributions were calculated assuming thermally insulating walls.

$$u = \frac{Gr}{Ha^2}\left(\frac{\sinh(Ha\,z)}{2\sinh(Ha/2)} - z\right). \tag{9}$$

Equation (8b) then yields:

thermally insulating walls

$$\vartheta = \varepsilon x + \frac{Pr_T\,\varepsilon\,Gr}{Ha^2}\left[\frac{1}{2Ha^2}\frac{\sinh(Ha\,z)}{\sinh(Ha/2)} - \frac{z^3}{6} + \left(\frac{1}{8} - \frac{\cosh(Ha/2)}{2\,Ha\sinh(Ha/2)}\right)z\right]; \tag{10}$$

thermally conducting walls

$$\vartheta = \varepsilon x + \frac{Pr_T\,\varepsilon\,Gr}{Ha^2}\left[\frac{1}{2\,Ha^2}\frac{\sinh(Ha\,z)}{\sinh(Ha/2)} - \frac{z^3}{6} + \left(\frac{1}{24} - \frac{1}{Ha^2}\right)z\right]. \tag{11}$$

3.2. *Analysis of the results*

3.2.1. *Check of validity.* In the low $Ha$ limit, a power series expansion of equation (9) keeping only the third order terms in $Ha$ gives

$$u = \frac{Gr}{6}(z^3 - z/4). \tag{12}$$

As for temperature, the fifth order terms have to be taken into account, and the results are:

thermally insulating walls

$$\vartheta = \varepsilon x + Pr\,\varepsilon\,Gr\left[\frac{z^5}{20} - \frac{z^3}{24} + \frac{z}{64}\right]; \tag{13}$$

thermally conductive walls

$$\vartheta = \varepsilon x + Pr\,\varepsilon\,Gr\left[\frac{z^5}{20} - \frac{z^3}{24} + \frac{7}{960}z\right]. \tag{14}$$

Equations (12)–(14) are identical to those obtained by Hart [12] in the absence of a magnetic field. It is indeed reassuring to see that equations (9)–(11) reach correct limits when the Hartmann number tends towards 0.

3.2.2. *Maximum velocity.* Figure 2 shows the variation of the maximum velocity as a function of the Hartmann number; it is seen that in the high $Ha$ range the decrease follows an $Ha^{-2}$ power law. Indeed, taking the derivative of equation (9) yields for the extremum:

$$z_0 = \frac{1}{Ha}\operatorname{argcosh}\left(\frac{2\sinh(Ha/2)}{Ha}\right) \tag{15}$$

which as $Ha$ tends towards infinity reduces to

$$z_0 = \frac{1}{2} + \frac{\log(2/Ha)}{Ha}$$

the result for maximum velocity is then

$$|u_M| = \tfrac{1}{2}Gr\,Ha^{-2}. \tag{16}$$

It can thus be said, as noted in ref. [1], that the group of non-dimensional parameters $u_M Ha^2/Gr$ governs convection in the fluid in the high $Ha$ limit, whereas $u_M/Gr$ plays a similar role in the non-magnetic problem [12].

3.2.3. *Velocity profiles.* Plots of $u/|u_M|$ are given in Fig. 3 for various values of $Ha$. For low values of $Ha$, the profile is simply cubic [12, 14] but as $Ha$ increases, the velocity gradient tends to be constant almost everywhere in the cavity. This is readily seen in equation (8a): in the high $Ha$ range, the $Ha^2\,du/dz$ term prevails except in the two thin Hartmann layers of thickness $Ha^{-1}$ near the walls, where the effect of viscosity cannot be neglected.

Furthermore, the interested reader will check that in the high $Ha$ limit, the velocity profiles of equation (9) can be split into two contributions:

(a) a core velocity $u_c$ valid when $1/2 - |z| \gg Ha^{-1}$

$$u_c = -\frac{Gr}{Ha^2}z; \tag{17a}$$

(b) the classical Hartmann exponential profiles [16]

$$u_{Ha} = u_c[1 - \exp\{\pm Ha(z \pm 1/2)\}]. \tag{17b}$$

As opposed to the case of pressure driven flows in ducts, the rotational of the Lorentz force in the core does not vanish due to the presence of the buoyancy

term in equation (2). Indeed, it is easy to check that in our problem, we now have $d^2u_c/dz^2 = 0$; as opposed to the pressure driven case (for which $u_c$ had to be uniform), here we find an example where the velocity gradient in the core must be constant.

3.2.4. *Temperature.* A glance at equations (10) and (11) ensures that the maximum values for both thermal boundary conditions also follow an $Ha^{-2}$ power law in the high $Ha$ range, but as $Ha$ tends towards infinity, the limits for equations (10) and (11) take simple forms:

thermally insulating walls

$$\vartheta = \varepsilon x + \frac{Pr\,\varepsilon\,Gr}{Ha^2}\left(-\frac{z^3}{6}+\frac{z}{8}\right); \tag{18}$$

thermally conducting walls

$$\vartheta = \varepsilon x + \frac{Pr\,\varepsilon\,Gr}{Ha^2}\left(-\frac{z^3}{6}+\frac{z}{24}\right). \tag{19}$$

The polynomials of equations (18) and (19) obviously do not lead to a boundary layer behaviour in the vicinity of the walls. Indeed, the temperature distribution (for thermally insulating walls) normalized with respect to their maximum values is also shown in Fig. 3 for several values of the Hartmann number; there is no significant difference in the shapes of the curves when $Ha$ increases.

3.2.5. *Electric current.* Going back to dimensional variables, equation (4) gives $\mathbf{j} = -\sigma B_0 U(Z)\mathbf{y}$; $\mathbf{j}$ thus flows in the positive (resp. negative) $Y$-direction in the upper (resp. lower) part of the cavity, with its lines closing at infinity. $U$ being an odd function of $Z$, it is clear that there is no net electric current across the $(X, Z)$ plane and that, as opposed to the classical Hartmann flow [17], there is no current recirculation through the Hartmann layers at the top and the bottom of the cavity. However, it has to be mentioned that the end effects in the $Y$-direction could have a major impact on the local velocities.

3.2.6. *Concluding remarks.* The same results could have been obtained through a different formulation of this 1D problem [18]. We could have assumed that the induced magnetic field $\mathbf{b}$, a function of $Z$ only, lies in the $X$-direction; a convecto-diffusive equation for $\mathbf{b}$ along with Ampere's law could then lead to the same set of equations for velocity and temperature. It is also interesting to notice the formal analogy between our results and those of the fluctuating gravity problem ($g$-jitters) [19]. In both cases, the additional linear term in equation (8a) tends to damp the buoyancy driven convective flow.

## 4. THE RECIRCULATING FLOW

### 4.1. *Further hypothesis*

For a crystal grower interested in solute segregation, the above 1D velocity field is not enough; indeed, what is of the utmost importance is the recirculation of the flow in front of the solid–liquid interface (the cold wall of our cavity). The reason is that, in a typical solidification run, the local convective movements play a key role in species transport in the melt. We will thus attempt to find a solution to equations (1)–(4); however, since the problem is now fully two-dimensional, a few restrictive assumptions have to be made.

First of all, we now consider an open, semi-infinite cavity submitted to a constant temperature gradient. In other words, we suppose that convective heat transfer is negligible. To support this hypothesis, it can be seen from equations (18) and (19) that in the high $Ha$ range, the distortion of the thermal field is indeed very small, especially in the case of low Prandtl number fluids (e.g. metals and semiconductors). Furthermore, we drop the non-linear inertial term $\mathbf{V}\cdot\nabla\mathbf{V}$. This can only be justified if the interaction parameter, the ratio of the Lorentz force to the inertial force, is very high with respect to unity. Intuitively, we expect that high $Ha$ again favour this condition, but we will come back later to check the validity of this assumption.

In order to satisfy the continuity equation, we look for a solution in terms of a non-dimensional stream function $\psi$ such that

$$u = \partial\psi/\partial z \quad w = -\partial\psi/\partial x \tag{20}$$

where $w$ is now the velocity component on the $z$-axis. Taking the rotational of equation (2) and inserting the above definition, we get for the variations of $\psi$:

$$\Delta^2\psi - Ha^2\,\partial^2\psi/\partial z^2 = Gr. \tag{21}$$

Let us look for a solution in the form of a series expansion:

$$\psi = \sum_0^\infty v_j(x)\cos\alpha_j z, \tag{22}$$

the $\alpha_j$ being given by $\alpha_j = (2j+1)\pi$ in order to ensure $\psi = 0$ at $z = \pm 1/2$. Clearly, with this choice $u = \partial\psi/\partial z$ does not vanish on the lateral walls of the cavity. However, as was done in the core problem, the classical correction of the velocity distribution within the Hartmann layers [16] can again be used to satisfy the no-slip conditions at $z = \pm 1/2$, at least when $Ha \gg 1$. We thus expect our assumption to be physically sound in the high $Ha$ range. For $v_j(x)$, the boundary conditions are:

$$v_j(x) = v_j'(x) = 0 \quad \text{at} \quad x = 0 \tag{23}$$

to ensure that both $u$ and $w$ vanish on the cold wall.

### 4.2. *Outline of the solution*

To start with, let us write the series expansion of $Gr$:

$$Gr = \sum_0^\infty g_j\cos\alpha_j z, \quad g_j = 4\frac{(-1)^j}{\alpha_j}Gr. \tag{24}$$

Using equations (22) and (24), equation (21) becomes

$$v_j^{(4)} - 2\alpha_j^2 v_j^{(2)} + (\alpha_j^4 + Ha^2\alpha_j^2)v_j = g_j. \tag{25}$$

To get the general solution in terms of $v_j$, we need to solve the algebraic equation

$$m^4 - 2\alpha_j^2 m^2 + (\alpha_j^4 + Ha^2\alpha_j^2) = 0.$$

Tedious but simple calculations lead to $m = \pm a_j \pm ib_j$ ($i^2 = -1$), $a_j$ and $b_j$ being given as

$$a_j = \frac{1}{2^{1/2}}[\alpha_j^2 + \alpha_j(Ha^2+\alpha_j^2)^{1/2}]^{1/2} \quad (26a)$$

$$b_j = \frac{1}{2^{1/2}}[-\alpha_j^2 + \alpha_j(Ha^2+\alpha_j^2)^{1/2}]^{1/2}. \quad (26b)$$

The general solution of equation (25) can then be written as

$$v_j(x) = \lambda_j e^{-a_j x}\cos b_j x + \mu_j e^{-a_j x}\sin b_j x + \nu_j e^{a_j x}\cos b_j x + \pi_j e^{a_j x}\sin b_j x + g_j/(\alpha_j^4 + Ha^2\alpha_j^2). \quad (27)$$

To ensure that $v_j$ remains bounded as $x$ tends towards infinity, we have to set $\nu_j = \pi_j = 0$. The boundary conditions of equation (23) are then:

$$\lambda_j + g_j/(\alpha_j^4 + Ha^2\alpha_j^2) = 0,$$
$$-\lambda_j a_j + \mu_j b_j = 0.$$

To sum up the results, we finally get

$$v_j(x) = \lambda_j[e^{-a_j x}\cos b_j x - 1] + \mu_j e^{-a_j x}\sin b_j x \quad (28a)$$

$$\lambda_j = -g_j/(\alpha_j^4 + Ha^2\alpha_j^2),$$
$$\mu_j = -a_j g_j/b_j(\alpha_j^4 + Ha^2\alpha_j^2). \quad (28b)$$

4.3. *Analysis of the results*

4.3.1. *Check of validity.* As opposed to the core problem, we do not have an analytical solution without a magnetic field to check the validity of our calculations. Worse, it would not serve out purpose to solve the simpler equation $\Delta^2\psi = Gr$; the mathematical result would not be physically relevant since in that inertialess, non-magnetic formulation, viscosity would govern momentum transfer throughout the cavity. In that case, dropping the no-slip conditions for $u$ on $z = \pm 1/2$ would be very dangerous. However, we can check the consistency of our 2D approach with respect to the core solution in the high $Ha$ range. Taking the limit of equation (28a) as $x$ tends towards infinity, we get

$$v_j(x) \to v_j^\infty = g_j/(\alpha_j^4 + Ha^2\alpha_j^2)$$

and consequently

$$\psi(x,z) \to \psi^\infty(z) = \sum_0^\infty g_j \cos\alpha_j z/(\alpha_j^4 + Ha^2\alpha_j^2).$$

Since both $\lambda_j$ and $\mu_j$ have $\alpha_j^4 + Ha^2\alpha_j^2$ terms at their denominator (see equations (28b)), we can expect that when $j$ gets high, the corresponding contribution will be quite small. If we now suppose that each $\alpha_j$ playing a significant role in the series is much smaller than $Ha$ (we will come back later to the domain of validity of this 'high $Ha$' approximation), we get

$$\psi^\infty = \frac{1}{Ha^2}\sum_0^\infty g_j \cos\alpha_j z/\alpha_j^2$$

with

$$g_j = 4\frac{(-1)^j}{\alpha_j}Gr.$$

After simple algebraic manipulations, the above series finally reduces to

$$\psi^\infty(z) = -\frac{Gr}{2\,Ha^2}(z^2 - 1/4).$$

Thus, far from the cold wall, the velocity component on the $x$-axis is

$$u^\infty = -\frac{Gr}{Ha^2}z. \quad (29)$$

Having dropped the no-slip conditions on the upper and lower walls, we cannot expect to fall back exactly on equation (9); it is, however, reassuring to see that both results are indeed equal everywhere except in the vicinity of $z = \pm 1/2$.

4.3.2. *Velocity profiles.* From a crystal grower point of view, velocity profiles are easier to handle than current functions. We will begin with the study of $w$, the component running down the cold wall. Using our series expansion, we can write:

$$w = -\sum_0^\infty v_j'(x)\cos\alpha_j z.$$

The first and second derivatives of $v_j$ are, respectively, according to equations (28)

$$v_j'(x) = -(\lambda_j b_j + \mu_j a_j)e^{-a_j x}\sin b_j x \quad (30a)$$

$$v_j^{(2)}(x) = -(\lambda_j b_j + \mu_j a_j) \times e^{-a_j x}[-a_j \sin b_j x + b_j \cos b_j x]. \quad (30b)$$

$v_j'$ reaches its maximum at $x_{0,j}$ such that

$$\tan b_j x_{0,j} = b_j/a_j.$$

To gain more insight into the physics of the problem, let us now focus on the high $Ha$ limit. Assuming again that each $\alpha_j$ playing a significant role in the series is much smaller than $Ha$, we get the asymptotic formulae:

$$a_j \simeq b_j \simeq \left(\frac{\alpha_j Ha}{2}\right)^{1/2} \quad (31a)$$

$$\lambda_j \simeq \mu_j \simeq -4\frac{Gr}{Ha^2}\frac{(-1)^j}{\alpha_j^3}. \quad (31b)$$

Thus the asymptotic values for $x_{0,j}$ and the maximum of $v_j'$ (in the following referred to as $v_{j,M}'$) are given by:

$$x_{0,j} = \frac{\pi}{4}\left(\frac{2}{\alpha_j Ha}\right)^{1/2} \quad (32a)$$

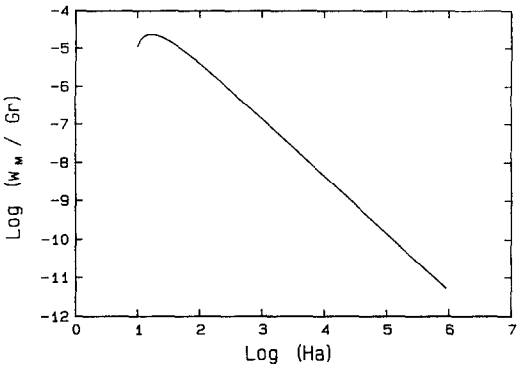


FIG. 4. Variation of the maximum of the $w$ component of velocity, normalized by $Gr$, as a function of $Ha$.

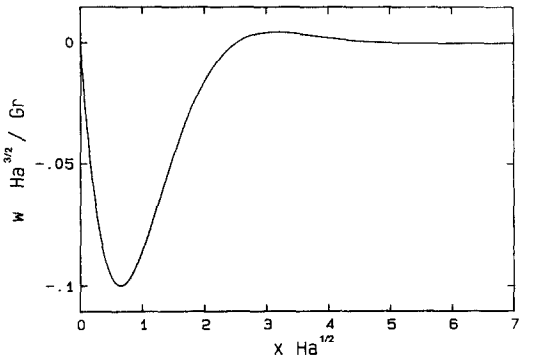


FIG. 6. Normalized $w$ velocity profile showing the variation of $(w\,Ha^{3/2})/Gr$ as a function of $x\,Ha^{1/2}$ in the middle of the cavity.

$$v'_{j,M} = -4\exp(-\pi/4)\frac{Gr}{Ha^{3/2}}\frac{(-1)^j}{\alpha_j^{5/2}}. \qquad (32b)$$

Thus, we expect the range of variation of $w$ and the associated length scale will follow asymptotic power laws in $Gr\,Ha^{-3/2}$ and $Ha^{-1/2}$ respectively in the high $Ha$ range. The above result can also be used to estimate the contribution of each term in the expansion: the ratio between $v_{j,M}$ and $v_{0,M}$ varies as $\alpha_j^{5/2}$, falling rapidly with $j$. For instance, at $j = 10$, $v_{j,M}/v_{0,M}$ is already smaller than $3 \times 10^{-5}$. We thus checked that truncation of the series at $j = 10$, 20 or 50 did not significantly change the final result in terms of $w$.

The curve giving the maximum value of $w$, $w_M$, as a function of $Ha$ is shown in Fig. 4. At high $Ha$, $w_M/Gr$ follows, as expected, an $Ha^{-3/2}$ power law (see Fig. 4); $(w_M\,Ha^{3/2})/Gr$ is then the relevant non-dimensional group for the study of the recirculating problem. Its variation with $Ha$, presented in Fig. 5, can be used to determine the range of validity of the high $Ha$ approximation. When this condition holds, say for $Ha > 100$, we also found that for each $z$, the $w(x)$ velocity profiles admitted a representation of the form $w\,Ha^{3/2}/Gr = f(x\,Ha^{1/2})$; the corresponding result is shown in Fig. 6 for the case $z = 0$ (middle of the cavity).

Again, using our series expansion, we can compute the $u$ component of velocity, given by

$$u = -\sum_0^\infty v_j(x)\,\alpha_j \sin\alpha_j z.$$

$u$ is seen to increase from 0 at $x = 0$ to a value $u_\infty$ given by equation (29) far away from the cold wall. We also checked that for each $z$, the $u(x)$ velocity profiles were self-similar in the high $Ha$ range. Since $a_j$ and $b_j$ are both of order of magnitude $Ha^{1/2}$, we expect that $Ha^{-1/2}$ will again be the relevant length scale in the recirculating area. This result is confirmed in Fig. 7, where we plotted the variation of $(u\,Ha^2)/Gr$ as a function of $x\,Ha^{1/2}$ at $z = 0.25$.

In all cases, we found numerically that $Ha$ greater than 100 ensured that the high $Ha$ approximation was valid. This is not unreasonable, since truncation of the expansion at $j = 10$ did not change the final result. We could have expected that the condition $\alpha_{10} \ll Ha$ was sufficient to guarantee this result.

4.3.3. *Self-consistency.* We can now come back on our assumption of high interaction parameter, i.e. the neglect of $\mathbf{V}\cdot\nabla\mathbf{V}$ in equation (2). Let us try to estimate the order of magnitude of the various non-dimensional inertial terms $u\partial u/\partial x$, $w\partial u/\partial z$, $u\partial w/\partial x$ and $w\partial w/\partial z$. The maximum values of $u$ and $w$ are in $Gr\,Ha^{-2}$ and $Gr\,Ha^{-3/2}$ and the associated length scales on $x$ and $z$ are $Ha^{-1/2}$ and 1, respectively. The leading contributions $u\partial w/\partial x$ and $w\partial w/\partial z$ then vary like $Gr^2\,Ha^{-3}$; this is to be compared with an estimate

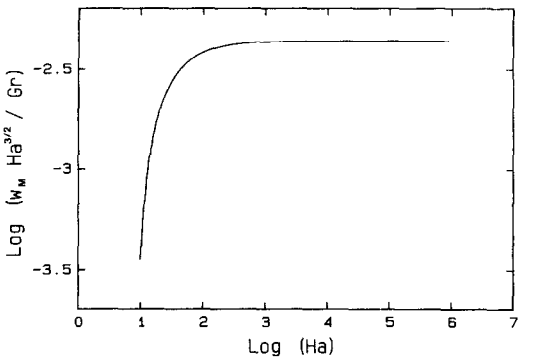


FIG. 5. Variation of the $(w_M\,Ha^{3/2})/Gr$ group that governs the recirculation as a function of $Ha$.

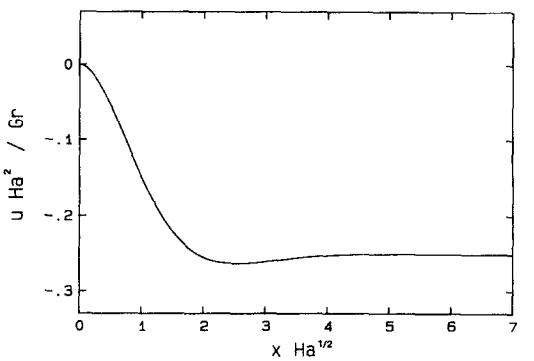


FIG. 7. Normalized $u$ velocity profile showing the variation of $(u\,Ha^2)/Gr$ as a function of $x\,Ha^{1/2}$ at $z = 0.25$.

for the Lorentz force, $Ha^2\,u$, of order of magnitude $Gr$. A condition for inertia to be negligible is thus

$$Ha^3/Gr \gg 1. \tag{33}$$

This condition can hold in usual horizontal Bridgman growth conditions where typical values of $Ha$ and $Gr$ are of order of magnitude 100 and $10^5$. Furthermore, if we refer to the non-magnetic problem [12], inertia is seen to play a minor role, even when the corresponding order of magnitude condition ($Gr \ll 1$) is not verified. Thus we do not expect our neglect of the $\mathbf{V}\cdot\nabla\mathbf{V}$ term to jeopardize the validity of our results.

Finally, due to the limited super-velocity observed in the recirculating area, convection can be expected to play a minor role in overall heat transfer in the high $Ha$ range. We thus think that our assumption of constant temperature gradient, that holds *stricto sensu* only for $Pr = 0$, is valid in most cases, at least for metals and semiconductors.

## 5. CONCLUSION

The purpose of this work was to propose a solution to the equations of magneto-hydrodynamics in order to study the effect of a transverse magnetic field on buoyancy driven convection in a two-dimensional cavity. One of the main features of the problem is that the electric field vanishes everywhere. Since the $x$-velocity profiles are odd functions of $z$, the current lines can be considered to be close at infinity, with no impact in our solution. However, one should bear in mind that 3D end effects in the $y$-direction could have a drastic influence on the local velocity field.

In the core problem, when the Hartmann number gets high, both velocity and temperature follow an $Ha^{-2}$ power law. Moreover, the velocity gradient $du/dz$ is seen to be constant everywhere in the cavity except in the two Hartmann layers of extent $Ha^{-1}$ near $z = \pm 1/2$ where the effect of viscosity becomes important. However, as opposed to what can be seen in the case of pressure driven flows in ducts, these boundary layers do not play a role in the recirculation of the current; their purpose is only to ensure that velocity vanishes at the wall.

To study the recirculating part of the flow, we were led to further simplifications. The effect of both convective heat transfer and inertia were supposed a priori negligible, but we came back later to check the validity of these assumptions. A boundary layer of extent $Ha^{-1/2}$ parallel to the cold wall is observed in the high $Ha$ limit. Both components of velocity $u$ and $w$ are seen to vary as $Gr\,Ha^{-2}$ and $Gr\,Ha^{-3/2}$ over this length scale.

We hope that this solution can be used to study solute repartition in a typical horizontal Bridgman growth experiment. It should be possible to derive a criterion giving, at a given $Gr$, the $Ha$ necessary to reach the diffusion controlled solidification conditions. Further extensions of this work could include the effect of confinement in the $y$-direction, thus yielding a full three-dimensional solution of the problem; a study of the stability of this solution in order to find the first threshold of non-stationarity would also be of interest.

*Acknowledgement*—The present work was conducted within the framework of the GRAMME agreement between the CNES and the CEA.

## REFERENCES

1. C. Vives and C. Perry, Effects of magnetically damped convection during the controlled solidification of metals and alloys, *Int. J. Heat Mass Transfer* **30,** 479–496 (1987).
2. H. P. Utech and M. C. Flemmings, Elimination of solute banding in indium antimonide crystals by growth in a magnetic field, *J. Appl. Phys.* **37,** 2021–2024 (1966).
3. L. N. Hjellming, A thermal model for Czochralski silicon crystal growth with an axial magnetic field, *J. Crystal Growth* **104,** 327–344 (1990).
4. T. Munakata and I. Tanasawa, Onset of oscillatory flow in a Czochralski growth melt and its suppression by magnetic field, *J. Crystal Growth* **106,** 566–576 (1990).
5. P. Sabhapathy and M. E. Salcuedan, Numerical study of flow and heat transfer in LEC growth of GaAs with an axial magnetic field, *J. Crystal Growth* **104,** 371–388 (1990).
6. R. Cartwright, O. J. Ilegbusi and J. Szekely, A comparison of order of magnitude and numerical analyses of flow phenomena in Czochralski and magnetic Czochralski systems, *J. Crystal Growth* **94,** 321–333 (1989).
7. W. E. Langlois, L. N. Hjellming and J. S. Walker, Effects of the finite electrical conductivity of the crystal on hydromagnetic Czochralski flow, *J. Crystal Growth* **83,** 51–61 (1987).
8. W. E. Langlois and K. J. Lee, Czochralski crystal growth in an axial magnetic field: effects of Joule heating, *J. Crystal Growth* **62,** 481–486 (1983).
9. S. Motakef, Magnetic field elimination of convective interference with segregation during vertical Bridgman growth of doped semiconductors, *J. Crystal Growth* **104,** 833–850 (1990).
10. H. Ozoe and K. Okada, The effect of the direction of the external magnetic field on the three dimensional convection in a cubical enclosure, *Int. J. Heat Mass Transfer* **32,** 1939–1954 (1989).
11. G. M. Oreper and J. Szekely, The effect of an external imposed magnetic field on buoyancy driven flow in a rectangular cavity, *J. Crystal Growth* **64,** 505–515 (1983).
12. J. E. Hart, Stability of thin non-rotating Hadley circulations, *J. Atmos. Sci.* **29,** 687–697 (1972).
13. J. E. Hart, Low Prandtl convection between differentially heated end walls, *Int. J. Heat Mass Transfer* **26,** 1069–1074 (1983).
14. R. V. Birikh, Thermocapillary convection in a horizontal layer of liquid, *J. Appl. Mech. Tech. Phys.* **3,** 69–72 (1966).
15. J. C. R. Hunt, Magnetohydrodynamic flow in rectangular ducts, *J. Fluid Mech.* **21,** 577–590 (1965).
16. R. Moreau, *Magnetohydrodynamics*, Chap. 4. Kluwer, Dordrecht (1990).
17. J. A. Shercliff, Steady motion of conducting fluids in pipes under transverse magnetic fields, *Proc. Camb. Phil. Soc.* **49,** 136–144 (1953).
18. J. P. Garandet, CEA Internal Report, DEM 90/01 (1990).
19. D. Thevenard and H. Ben Hadid, Low Prandtl number convection in a rectangular cavity with longitudinal thermal gradient and transverse $g$-jitters, *Int. J. Heat Mass Transfer* **34,** 2167–2173 (1991).

## CONVECTION NATURELLE DANS UNE CAVITE RECTANGULAIRE AVEC CHAMP MAGNETIQUE TRANSVERSE

**Résumé**—Nous proposons une solution analytique aux équations de la magnétohydrodynamique permettant de modéliser l'effet d'un champ magnétique transverse sur la convection thermique dans une cavité bidimensionnelle. Dans la limite des nombres de Hartmann élevés, le gradient de vitesse dans le coeur de l'écoulement est constant sauf dans les deux couches de Hartmann au voisinage des parois normales au champ magnétique. Nous montrons que cette solution de coeur est applicable partout à l'exception d'une couche limite d'étendue $Ha^{-1/2}$ à proximité du mur froid. La partie recirculante de l'écoulement est étudiée à l'aide d'un développement en série qui permet de calculer la fonction de courant. Nous présentons également la variation des deux composantes de la vitesse en fonction de $Ha$ ainsi qu'une discussion de la validité de nos hypothèses.

## NATÜRLICHE KONVEKTION IN EINEM RECHTECKIGEN HOHLRAUM UNTER DEM EINFLUSS EINES QUERLIEGENDEN MAGNETFELDES

**Zusammenfassung**—Es wird eine analytische Lösung der magneto-hydrodynamischen Gleichungen vorgestellt, mit deren Hilfe man den Einfluß eines querliegenden Magnetfeldes auf die natürliche Konvektion in einem zweidimensionalen Hohlraum beschreiben kann. An der oberen Grenze der Hartmann-Zahl ist der Geschwindigkeitsgradient im Kern konstant-dies gilt außerhalb der beiden Hartmann-Schichten in der Nähe der senkrecht vom Magnetfeld durchquerten Wände. Es wird gezeigt, daß diese Kern-Lösung an jeder Stelle des Hohlraums gilt, mit Ausnahme einer Grenzschicht der Dicke $Ha^{-1/2}$ an der kalten Wand. Der rezirkulierende Teil der Strömung wird mit Hilfe einer Reihenentwicklung untersucht, mit deren Hilfe die Berechnung der Stromfunktion möglich ist. Abschließend wird der Einfluß der Kennzahl $Ha$ auf die beiden Geschwindigkeitskomponenten gezeigt, und die Gültigkeit der getroffenen Annahmen wird diskutiert.

## КОНВЕКЦИЯ, ВЫЗВАННАЯ ПОДЪЕМНОЙ СИЛОЙ, В ПРЯМОУГОЛЬНОЙ ПОЛОСТИ С ПОПЕРЕЧНЫМ МАГНИТНЫМ ПОЛЕМ

**Аннотация**—Предложено аналитическое решение уравнений магнитогидродинамики, которое может использоваться при моделировании влияния поперечного магнитного поля на вызванную подъемной силой конвекцию в двумерной полости. В пределе высоких чисел Хартманна градиент скорости в ядре является постоянным вне обоих слоев Хартманна возле стенок, перпендикулярных магнитному полю. Показано, что решение для ядра справедливо во всей полости за исключением пограничного слоя толщиной $Ha^{-1/2}$ у ненагретой стенки. Рециркулирующая часть течения исследуется методом разложения в ряд, что позволяет вычислить функцию тока. Описывается также изменение обеих компонент скорости как функций $Ha$ и обсуждается правомерность используемых допущений.